ACCOUNTS
of chemical research

Reactions of Aromatic N-Heterocycles with d^0f^n-Metal Alkyl Complexes Supported by Chelating Diamide Ligands

PAULA L. DIACONESCU*
Department of Chemistry & Biochemistry, University of California, Los Angeles, California 90095

RECEIVED ON APRIL 5, 2010

CONSPECTUS

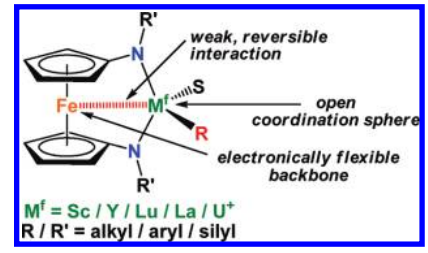

Aromatic heterocycles are a prominent feature within natural products and pharmaceuticals and considerable efforts are directed toward their synthesis and functionalization. These molecules also appear as unwanted impurities in carbon-based fuels, and processes that fragment them are of increasing interest. Early transition metal−carbon bonds show diverse reactivity toward aromatic heterocycles: researchers have reported both functionalization, relevant to synthetic efforts, and ring opening, relevant to their removal from fuels. In particular, chelating ferrocene−diamides possess unique electronic characteristics as ancillary ligands that enable a wide range of reactivity behaviors for the resulting metal complexes. In this Account, we describe our efforts to understand the reactivity of group 3 metal and uranium alkyl complexes supported by these organometallic ligands toward aromatic N-heterocycles.

Two geometrically related ancillary ligands were investigated: 1,1′-ferrocenylene−diamides and pincer-type pyridine−diamides. A substrate-dependent behavior was observed. For example, all the benzyl metal complexes cleaved 1-methylimidazole. In the case of pyridines, differences in reactivity were identified: C−H activation and C−C coupling occurred with substituted pyridines, while alkyl transfer predominated with isoquinoline and chelating pyridines. The products of the C−C coupling or the alkyl-transfer reactions underwent subsequent hydrogen transfer: within the same ring for the substituted pyridines and between two different heterocycles for isoquinoline and chelating pyridines.

The comparison between yttrium and lutetium benzyl complexes supported by ferrocene− or pyridine−diamide ligands indicated that similar reactions occurred for specific substrates (1-methylimidazole, 2-picoline, and isoquinoline). A broader range of reaction types and a larger substrate scope were identified, however, for the ferrocene than for the pyridine-type complexes.

Based on the reactions discussed in this Account and on isolated examples drawn from the literature, we conclude that the ferrocene−diamides represent a versatile ligand framework. We propose that iron's ability to accommodate changes in the electronic density at the metal center more readily than classical supporting ligands leads to the privileged status of these organometallic ancillary ligands.

A. Introduction

The relevance of aromatic heterocycles to natural products and pharmaceuticals has prompted a concerted research effort toward their synthesis and functionalization.[1] Aromatic heterocycles also appear as unwanted impurities in carbon-based fuels and, recently, processes that fragment them have become prominent.[2] Interestingly, early transition metal−carbon bonds show diverse reactivity toward these substrates: functionalization as well as ring-opening have been reported.[3] Herein we describe our efforts to understand the reactivity of group 3 metal and uranium alkyl complexes toward aromatic N-heterocycles. Most of the reactions discussed start with the C−H activation of the heterocycle, a complementary process to metalation reactions with main-group organome-

Published on the Web 07/21/2010 www.pubs.acs.org/acr
10.1021/ar1000605

CHART 1. Diamine Proligands Discussed

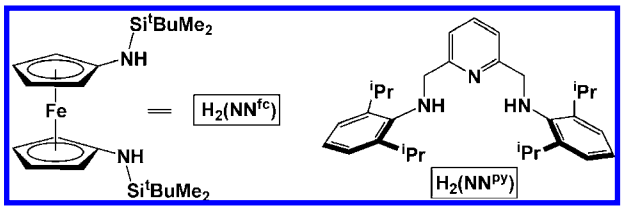

tallic reagents.[1] This Account begins by presenting the properties of a new class of d^{0}f^n-metal alkyl complexes supported by 1,1′-ferrocene−diamide ligands; the discussion follows with a description of the reactivity of these complexes toward aromatic N-heterocycles and ends with a comparison with the reactivity of analogous pyridine−diamide metal complexes.

B. Alkyl Complexes of d^{0}f^n Metals Supported by Chelating Diamide Ligands

The long-standing endeavors of organometallic chemistry at ligand design to modulate metal reactivity have been amplified in recent years by reports of direct ligand involvement in reactions.[4] Our initial goal was to synthesize electrophilic metal−alkyl complexes that would draw on such behavior and display new reactivity. 1,1′-Ferrocenylene−diamides (NN^{fc}, Chart 1) appeared to be desirable frameworks because of a number of characteristics:

(1) The 1,1′-disubstituted ferrocene enforces a *cis*-coordination of the two donors; thus, only one side of the d^{0}f^n metal center is blocked, leaving the other side open to attack by various substrates.
(2) The ferrocene backbone has the ability to accommodate changes in the electronic density at the metal center by varying the geometry around iron.
(3) A weak interaction of donor−acceptor type may occur between iron and the d^{0}f^n metal, possibly influencing the reactivity of the complex.
(4) The ligand backbone is redox active (this characteristic has yet to be fully investigated in relation to the reactivity of the resulting d^{0}f^n alkyl complexes).

The first feature proved important in stabilizing mononuclear complexes and allowing reactions with bulky substrates. A combination of characteristics 1 and 3 gives these ligands a close resemblance to pincer ligands; therefore, we also prepared the analogous complexes of 2,6-bis(2,6-diisopropylanilidomethyl)pyridine (NN^{py}, Chart 1) for comparison. The unique characteristics of the ferrocene-based ligands, however, are likely responsible for the plethora of new complexes and reaction outcomes observed.

SCHEME 1. Syntheses of Group 3 Metal Benzyl Complexes Supported by Ferrocene− and Pyridine−Diamide Ligands

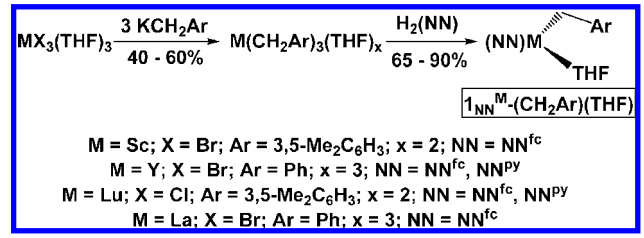

Two series of alkyl complexes were targeted: group 3 metal (scandium, yttrium, lutetium, and lanthanum) and uranium(IV) complexes. These two classes of compounds were of interest because (i) they incorporate highly electrophilic metal centers that would prove advantageous in reactions with unreactive functionalities and (ii) they encompass monoalkyl (group 3) and dialkyl (uranium) complexes. Uranium is especially interesting because the two alkyl groups can both engage in reactions with the same substrate (by comparison, group 4 metals require a transformation to alkyl cationic compounds in order to display reactivity similar to that shown by neutral group 3 metal or uranium complexes).

Ferrocene−diamide complexes were initially reported for group 4 metals by Arnold et al.,[5] who also showed that a highly reactive, cationic titanium(IV) species was stabilized by an interaction with the iron center.[6] Such interactions had been proposed earlier for late transition metals.[7] Recently, the Stephan group has reported that ferrocenyl can stabilize cyclopentadienyl group 4 metal alkyl cations through an iron−metal interaction.[8]

1. Synthesis of Alkyl Complexes. Group 3 metal benzyl complexes were synthesized by acid−base reactions from the corresponding tris(benzyl) compounds and the proligands H$_2$(NN^{fc}) (NN^{fc} = fc(NSi^{t}BuMe$_2$)$_2$, fc =1,1′-ferrocenylene) or H$_2$(NN^{py}) to give **1$_{fc}^M$-(CH$_2$Ar)(THF)** (Scheme 1; M = Sc, Lu, Ar = 3,5-Me$_2$C$_6$H$_3$; M = Y, La, Ar = Ph)[9−13] or **1$_{py}^M$-(CH$_2$Ar)(THF)** (Scheme 1; M = Y, Ar = Ph; M = Lu, Ar = 3,5-Me$_2$C$_6$H$_3$),[14] respectively. The syntheses of new scandium and yttrium tris(benzyl) complexes[9,10] were inspired by a report from Hessen et al.[15] on the synthesis of La(CH$_2$Ph)$_3$(THF)$_3$. These starting materials are less expensive than the alkyls commonly used[16] and eliminate mesitylene or toluene during the acid−base reactions, which is volatile and does not contaminate the desired product.[17]

The ferrocene−diamide uranium dialkyl complexes (Scheme 2) were synthesized by salt-metathesis reactions between the corresponding diiodide, **1$_{fc}^U$-I$_2$(THF)**, and various alkyl sources (benzyl potassium, neopentyl lithium).[18] The synthesis of **1$_{py}^U$-(CH$_2$Ph)$_2$** was accomplished in situ[19] since

SCHEME 2. Syntheses of Uranium Dibenzyl Complexes Supported by Ferrocene− and Pyridine−Diamide Ligands

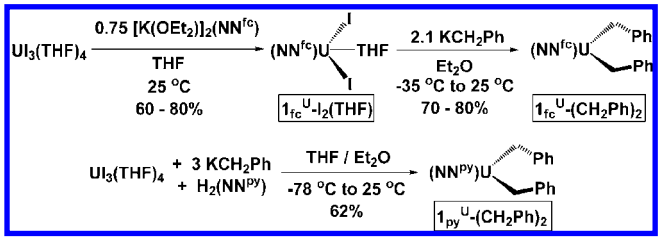

TABLE 1. Comparison of Iron−Metal Distances in d^0f^n-Metal Alkyl Complexes

entry	complex	X-ray Fe−M distance (Å)	sum of covalent radii (Å)	Δ_{Fe-M} (Å)	ref
1	$\mathbf{1_{fc}^{Sc}}$-(**CH$_2$Ar**)(**THF**)	3.16	3.02	+0.14	9
2	$\mathbf{1_{fc}^{Sc}}$-(**Me**)(**THF**)$_2$	3.26	3.02	+0.24	9
3	$\mathbf{1_{fc}^{Y}}$-(**CH$_2$Ph**)(**THF**)	3.24	3.22	+0.02	10
4	$\mathbf{1_{fc}^{Lu}}$-(**CH$_2$Ar**)(**THF**)	3.25	3.19	+0.06	11
5	$\mathbf{1_{Ad}^{Lu}}$-(**CH$_2$Ar**)(**DME**)	3.34	3.19	+0.15	13
6	$\mathbf{1_{Mes}^{Lu}}$-(**CH$_2$Ar**)(**THF**)	3.12	3.19	−0.07	this work
7	$\mathbf{1_{fc}^{La}}$-(**CH$_2$Ar**)(**THF**)	3.38	3.39	−0.01	12
8	$\mathbf{1_{fc}^{U}}$-(**CH$_2$Ph**)$_2$	3.19	3.28	−0.09	18
9	$\mathbf{1_{fc}^{U}}$-(**CH$_2$Ph**)(**OEt$_2$**)	3.07	3.28	−0.20	18

the salt-metathesis route did not lead to the desired pyridine−diamide diiodide complex. The in situ method proved general and allowed not only the isolation of pyridine−diamide dialkyl uranium(IV) complexes but also the isolation of other ferrocene−diamide complexes that had not been accessible by the salt-metathesis method.[19]

2. X-ray Characterization. The solid-state structures of all $\mathbf{1_{fc}^{M}}$-(**CH$_2$Ar**)(**THF**) complexes were determined by single-crystal X-ray diffraction. For uranium, both the dibenzyl $\mathbf{1_{fc}^{U}}$-(**CH$_2$Ph**)$_2$ and the benzyl cation [$\mathbf{1_{fc}^{U}}$-(**CH$_2$Ph**)(**OEt$_2$**)][**BPh$_4$**] were structurally characterized as well as the pyridine−diamide complex $\mathbf{1_{py}^{U}}$-(**CH$_2$Ph**)$_2$. With all the solid-state data in hand, a comparison of the iron−metal distances is possible (Table 1). For scandium, yttrium, and lutetium, the iron−metal distance is larger than the sum of the covalent radii[20] (entries 1−5), while for lanthanum and uranium, it is smaller (entries 7−9). This distance is responsive to the electronic makeup of the ligands, as shown by the substitution of the silyl by an adamantyl group in [fc(NAd)$_2$]Lu-(CH$_2$Ar)(DME) ($\mathbf{1_{Ad}^{Lu}}$-(**CH$_2$Ar**)(**DME**), Ad = 2-adamantyl), causing this distance to increase (entry 5) or by a mesityl group in [fc(NMes)$_2$]Lu(CH$_2$Ar)(THF) ($\mathbf{1_{Mes}^{Lu}}$-(**CH$_2$Ar**)(**THF**), Mes =2,4,6-Me$_3$C$_6$H$_2$), causing this distance to decrease (entry 6). The presence of two instead of one ether donors also causes the iron−metal distance to increase (entries 1,2 and 4,5).

SCHEME 3. Ring Opening of 1-Methylimidazole Mediated by the Group 3 Metal Benzyl Complexes $\mathbf{1_{fc}^{M}}$-(**CH$_2$Ar**)(**THF**)

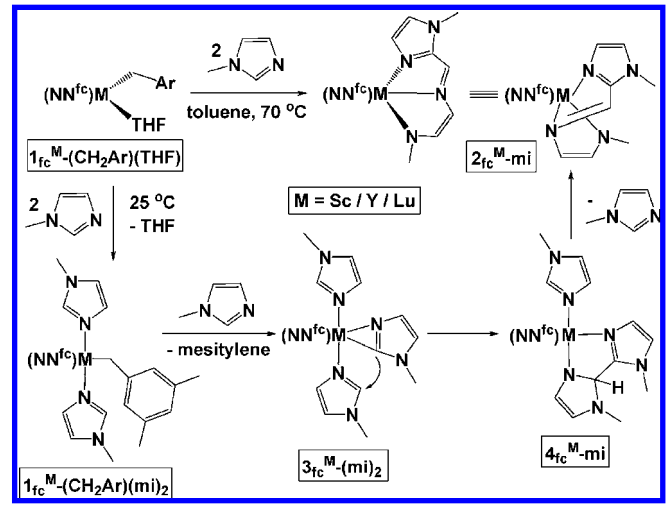

C. Reactions with Aromatic N-Heterocycles

The Hirshfeld charges calculated for M in $\mathbf{1_{fc}^{M}}$-(**CH$_2$Ar**)(**THF**) (see section D) are similar to those found for Cp*$_2$M(CH$_2$Ph) (M = Sc, 0.49, and 0.45 for Cp*$_2$Sc(CH$_2$Ph)(THF); M = Y, 0.58). All group 3 metal benzyl complexes coordinate THF. In order to compare their reactivity to that of the analogous metallocenes, reactions with aromatic N-heterocycles, which can displace the coordinated THF, were studied. Since [Cp*$_2$ZrMe(THF)]$^+$ did not C−H activate 1-methylimidazole (only coordination was observed),[21] the reactions of this substrate toward the group 3 metal and uranium alkyl complexes were studied first.

1. Reactions with Imidazoles. The reaction mixture obtained from $\mathbf{1_{fc}^{Sc}}$-(**CH$_2$Ar**)(**THF**) and 3 equiv of 1-methylimidazole (mi, Scheme 3) turned, surprisingly, from yellow or light orange to a dark-purple color after it was heated for several hours at 70 °C. The isolated product was characterized as $\mathbf{2_{fc}^{Sc}}$-**mi** and contained an imidazole−imine−amide moiety, in which one imidazole fragment was ring opened. Other examples of homogeneous systems that mediate the ring opening of aromatic N-heterocycles are also based on early transition metals, such as tantalum,[22] niobium,[23,24] and titanium,[25,26] with the exception of a rhenium system,[27,28] which employs external bases and electrophilic reagents, and of a low-valent tungsten complex that breaks the C−C bond of quinoxaline.[29] Actinide complexes also effect the ring opening of aromatic N-heterocycles, as reported by the Kiplinger group for thorium and pyridine-*N*-oxides[30] and by the Gambarotta group, when redox processes contribute to pyrazole ring opening by uranium centers.[31]

The ring opening of 1-methylimidazole was found to be mediated by all $\mathbf{1_{fc}^{M}}$-(**CH$_2$Ar**)(**THF**) complexes.[10,11] The following mechanism was proposed based on NMR spectroscopy

SCHEME 4. Reactions of 1-Methylbenzimidazole with $\mathbf{1_{fc}^{M}}$-(**CH$_2$Ar**)(**THF**) (M = Y, Lu)

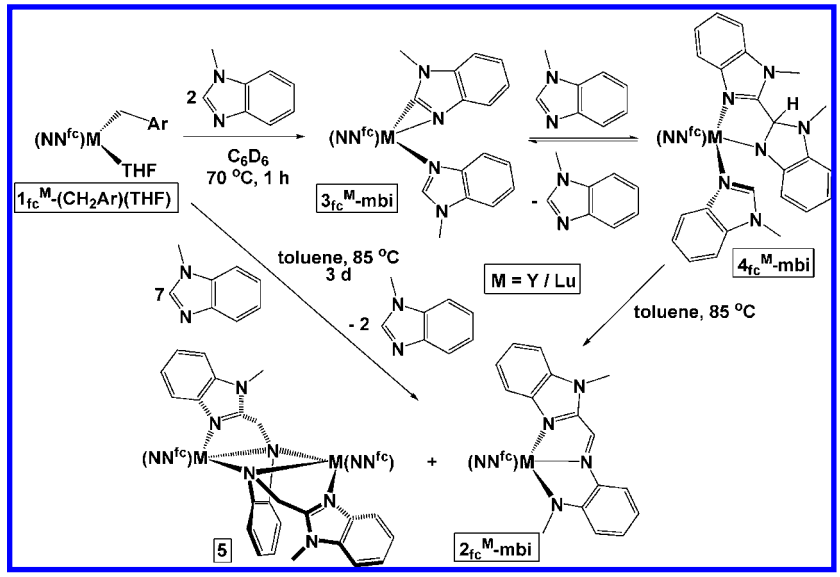

and X-ray crystallography studies (Scheme 3):[11] the first step involves displacement of THF and coordination of two imidazole molecules. The C−H activation of one of the 1-methylimidazole ligands to give $\mathbf{3_{fc}^{M}}$-(**mi**)$_2$ is the slow step of the entire process. This is consistent with the fact that $[Cp_2ZrMe(THF)]^+$ did not promote C−H activation of 1-methylimidazole.[21] Following C−H activation, C−C coupling[32] between the η^2-N,C-imidazolyl and one of the coordinated imidazoles occurs and is accompanied by the dearomatization of one of the rings to give $\mathbf{4_{fc}^{M}}$-**mi**. That intermediate was not observed; it was proposed that it transformed into the final product, $\mathbf{2_{fc}^{M}}$-**mi**, likely stabilized by extended conjugation. The complex $\mathbf{1_{fc}^{M}}$-(**CH$_2$Ar**)(**mi**)$_2$ was characterized for all metal centers by ^{1}H NMR spectroscopy, and the C−H activated complex was crystallographically characterized for $\mathbf{3_{fc}^{Y}}$-(**mi**)$_2$.[10] The above mechanistic scheme was supported by DFT calculations.[11] In addition to providing information about the ring-opening step, the calculations revealed that the dearomatized 1-methylimidazole fragment must undergo a rotation to allow the coordination of the nitrogen bearing the methyl group. This rotation showed the highest activation barrier of the intramolecular process.[11]

The reactions between $\mathbf{1_{fc}^{M}}$-(**CH$_2$Ar**)(**THF**) and 1-methylbenzimidazole (mbi) provided further support for the proposed mechanism.[33] Although the reaction with the scandium complex $\mathbf{1_{fc}^{Sc}}$-(**CH$_2$Ar**)(**THF**) led only to the isolation of the η^2-N,C-imidazolyl complex $\mathbf{3_{fc}^{Sc}}$-**mbi**, the reaction with the larger analogues, $\mathbf{1_{fc}^{M}}$-(**CH$_2$Ar**)(**THF**) (M = Y, Lu), allowed the observation of the C−C coupled product $\mathbf{4_{fc}^{M}}$-**mbi** (Scheme 4). Interestingly, the formation of the C−C bond in $\mathbf{4_{fc}^{M}}$-**mbi** was reversible, as shown by variable-temperature ^{1}H NMR spectroscopy and DFT calculations. The reversible event was also invoked to explain the formation of an unusual dinuclear product (**5**), assumed to result from the reaction of $\mathbf{2_{fc}^{M}}$-**mbi** and $\mathbf{4_{fc}^{M}}$-**mbi** by a complicated protonation/deprotonation reaction sequence.[33]

The reactivity of the uranium complex $\mathbf{1_{fc}^{U}}$-(**CH$_2$Ph**)$_2$ toward imidazoles was also studied. Based on the high electrophilicity of the uranium center and the fact that $\mathbf{1_{fc}^{U}}$-(**CH$_2$Ph**)$_2$ has two alkyl ligands, two molecules of substrate were expected to engage in C−H activation. Indeed, $\mathbf{1_{fc}^{U}}$-(**CH$_2$Ph**)$_2$ mediated the C−H activation of two heterocycles in the case of 1-methylimidazole (to give $\mathbf{6^{mi}}$-**mi**) or 1-methylbenzimidazole (to give $\mathbf{6^{mbi}}$-**mbi**). That process was followed by an unprecedented reaction cascade leading to the ring opening and functionalization of imidazoles (Scheme 5).[34] This double C−H activation and the sequence of transformations succeeding it are unique to uranium and have been observed for other aromatic heterocycles as well.[35]

For uranium, two isomeric products were isolated and characterized: **7A** and **7B**. Complexes **7A** and **7B** feature a new ligand formed from the coordinated imidazole and the two imidazolyl fragments initially present in $\mathbf{6^{mi}}$-**mi**: one C−N bond in the coordinated imidazole ring was broken, while the other two rings resemble the original imidazolyl entities. A proposed mechanism, based on the isolation of the 1-methylbenzimidazole C−C coupled product, $\mathbf{8^{mbi}}$, is reminiscent of the 1-methylimidazole ring opening by group 3 metal complexes. The novelty of the present process results from the ability of uranium to mediate an additional reaction, the migratory insertion of an imidazolyl ligand. Interestingly, the C−C coupling between the two imidazole rings in $\mathbf{8^{mbi}}$ was

SCHEME 5. Reactions of 1-Methylimidazole with $\mathbf{1_{fc}^{U}\text{-}(CH_2Ph)_2}$

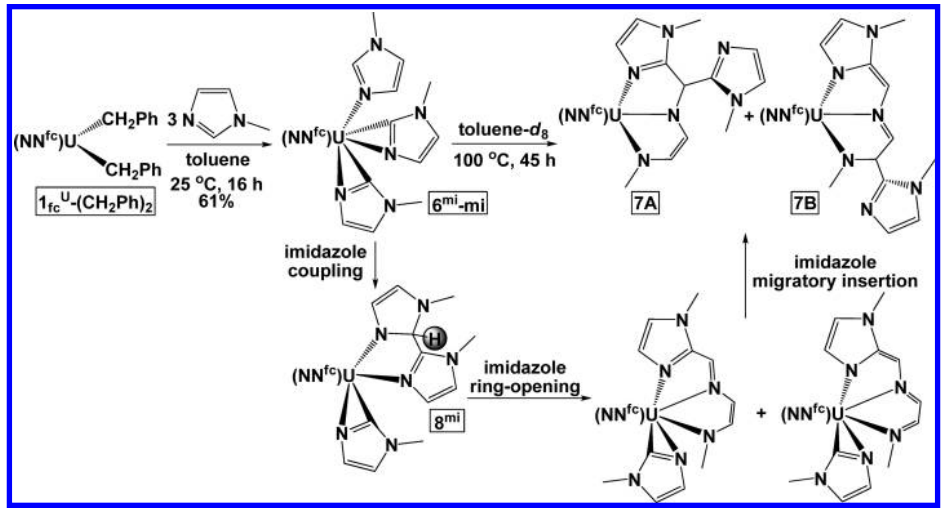

also found to be reversible,[36] as was the case for lutetium. The reversibility of the C−C coupling in $\mathbf{8^{mbi}}$ was supported by single-crystal and powder X-ray diffraction, ^{1}H and ^{2}H variable-temperature NMR spectroscopy, and DFT calculations.[36]

2. Reactions with Pyridines. i. C−H Activation. Since the largest part of nitrogen impurities in fuel is comprised of pyridine or pyrrole derivatives,[2] we became interested in extending the ring-opening reaction of imidazoles to pyridines. Pyridines were initially screened for C−H activation processes analogous to the first step in the ring opening of imidazoles. All benzyl complexes gave complicated reaction mixtures with the parent substrate,[11] but the scandium methyl complex $\mathbf{1_{fc}^{Sc}\text{-}(Me)(THF)_2}$ led to the expected C−H activated product, $\mathbf{9_{fc}^{M}\text{-}py}$.[37] If the pyridine was ortho-substituted, then the C−H activation reaction proceeded smoothly and gave the expected ortho-metalated products $\mathbf{9_{fc}^{M}}$ (Table 2).[38] When 2,6-lutidine was employed, a κ^3-N,C,C-coordination of lutidine ensued for the resulting methylene complex, $\mathbf{9_{fc}^{Sc}\text{-}lut}$ (Scheme 6). Interestingly, the C−H activation of 2-picoline by $\mathbf{1_{fc}^{M}\text{-}(CH_2Ph)(THF)}$ (M = Y, La) gave exclusively $\mathbf{9_{fc}^{M}\text{-}pic}$, featuring an sp^3-C_{CH_2}−M bond instead of an sp^2-$C_{pyridyl}$−M bond. Similar results have been reported for some yttrium[39] and thorium alkyl complexes.[40]

ii. Coupling. Next, the reactivity of the newly synthesized pyridyl complexes $\mathbf{9_{fc}^{M}}$ toward pyridines was investigated in order to determine whether C−C coupling occurs. As mentioned, the reaction between $\mathbf{1_{fc}^{M}\text{-}(CH_2Ar)(THF)}$ and excess pyridine gave a mixture of products; it was identified that the mixture showed signals in the olefinic region of its ^{1}H NMR spectrum. If ortho-substituted pyridines were employed, however, the C−C coupling reaction was remarkably general ($\mathbf{10_{fc}^{M}}$, Table 2).

TABLE 2. Coupling of Aromatic N-Heterocycles[a]

Compound	Substrate	Product
$\mathbf{9_{fc}^{M}\text{-}py^{Ph}}$		$\mathbf{10_{fc}^{M}\text{-}py^{Ph}\text{-}iqn^{Me}}$ M = Sc / Y / Lu
$\mathbf{9_{fc}^{Sc}\text{-}qn^{Me}}$		$\mathbf{10_{fc}^{Sc}\text{-}qn^{Me}\text{-}iqn^{Me}}$
$\mathbf{9_{fc}^{Sc}\text{-}py^{Ph}}$		$\mathbf{10_{fc}^{Sc}\text{-}py^{Ph}\text{-}phan}$
$\mathbf{9_{fc}^{Sc}\text{-}py^{Ph}}$		$\mathbf{10_{fc}^{Sc}\text{-}py^{Ph}\text{-}bipy}$
$\mathbf{9_{fc}^{Sc}\text{-}py^{Si}}$		$\mathbf{10_{fc}^{Sc}\text{-}py^{Si}\text{-}iqn^{Me}}$
$\mathbf{9_{fc}^{Sc}\text{-}bqn}$		$\mathbf{10_{fc}^{Sc}\text{-}bqn\text{-}phan}$
$\mathbf{9_{fc}^{Sc}\text{-}acr}$		$\mathbf{10_{fc}^{Sc}\text{-}acr\text{-}phan}$

[a] All reactions occurred in toluene or toluene/*n*-pentane at room temperature.

SCHEME 6. Coupling of Methylene− and Ethylene−Pyridine Complexes with 3-Methylisoquinoline

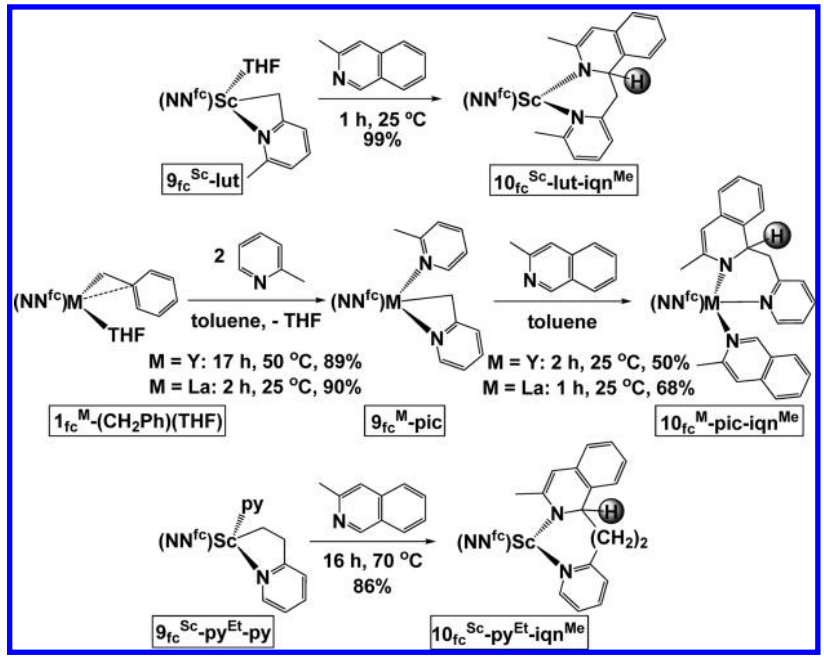

Several factors were found to promote the coupling reactions of the C−H activated complexes $\mathbf{9_{fc}^{M}}$ with pyridine substrates:[38]

(1) Ortho-substituents accelerated it, although large substituents inhibited it.
(2) The use of chelating substrates was beneficial.
(3) Fused aromatic rings on the coupling partner had an accelerating effect.

It became apparent that the coupling reaction was not restricted to η^2-N,C-pyridyl complexes when an analogous reaction was observed from the CH_2 group of $\mathbf{9_{fc}^{Sc}}$**-lut** (Scheme 6). The reaction of $\mathbf{9_{fc}^{Sc}}$**-lut** with 3-methylisoquinoline led to a coupled product, $\mathbf{10_{fc}^{Sc}}$**-lut-iqn**$^{\mathbf{Me}}$, in which the two heterocyclic rings were bridged by a methylene group. The formation of $\mathbf{10_{fc}^{Sc}}$**-lut-iqn**$^{\mathbf{Me}}$ was not an isolated example and the yttrium and lanthanum compounds obtained by the C−H activation of 2-picoline, $\mathbf{9_{fc}^{M}}$**-pic** (M = Y, La), also reacted with 3-methylisoquinoline to give $\mathbf{10_{fc}^{M}}$**-pic-iqn**$^{\mathbf{Me}}$. Furthermore, $\mathbf{9_{fc}^{Sc}}$**-py**$^{\mathbf{Et}}$**-py**, a compound that contains a Sc-CH_2CH_2-pyridine motif,[37] also reacted with 3-methylisoquinoline to give the coupling product $\mathbf{10_{fc}^{Sc}}$**-py**$^{\mathbf{Et}}$**-iqn**$^{\mathbf{Me}}$, in which the two heterocycles are bridged by a 1,2-ethylene group.[38]

In an attempt to determine whether the nucleophilic attack of an η^2-imidazolyl ligand would lead to the ring opening of other N-heterocycles and generalize the ring-opening reaction discussed earlier (Scheme 3), efforts were made to prepare solvates and coupled products starting from an (NN^{fc})Sc(η^2-N,C-imidazolyl) fragment. Although $\mathbf{3_{fc}^{Sc}}$**-mi** was isolated (Scheme 7), all attempts to produce a THF or a nonchelating pyridine solvate of (NN^{fc})Sc(η^2-N,C-imidazolyl) resulted in the formation of [(NN^{fc})Sc(μ^2,κ^2-N,C-2-(1-methylimidazolyl)]$_2$, $\mathbf{[3_{fc}^{Sc}]_2}$, in which the two scandium centers were bridged by two imidazolyl ligands (Scheme 7). Neither $\mathbf{3_{fc}^{Sc}}$**-mi** nor $\mathbf{[3_{fc}^{Sc}]_2}$ reacted with pyridines; however, both complexes reacted with 2,2′-bipyridine at 50 °C and yielded a bright red-orange coupled product, $\mathbf{10_{fc}^{Sc}}$**-mi-bipy** (Scheme 7). Attempts to identify a further transformation of $\mathbf{10_{fc}^{Sc}}$**-mi-bipy** by prolonged heating were not successful.

iii. Isomerization. In order to test the reactivity of the newly obtained pyridine-coupled products, C_6D_6 solutions of $\mathbf{10_{fc}^{M}}$**-py**$^{\mathbf{Ph}}$**-iqn** (M = Sc, Y, Lu) were heated at 70 or 85 °C for several days, during which time their color changed from red to green (Scheme 8). All $\mathbf{10_{fc}^{M}}$**-py**$^{\mathbf{Ph}}$**-iqn** compounds transformed with at least 60% conversion into $\mathbf{11_{fc}^{M}}$**-py**$^{\mathbf{Ph}}$**-iqn**, in which a different carbon of the dearomatized ring became sp^3.[11] The isomerization by 1,4-hydrogen transfer was also observed for the coupled product of 2-phenylpyridine with 2-picoline ($\mathbf{10_{fc}^{Sc}}$**-py**$^{\mathbf{Ph}}$**-pic**) or of 8-methylquinoline with 3-methylisoquinoline ($\mathbf{10_{fc}^{Sc}}$**-qn**$^{\mathbf{Me}}$**-iqn**$^{\mathbf{Me}}$), which transformed to $\mathbf{11_{fc}^{Sc}}$**-py**$^{\mathbf{Ph}}$**-pic** and $\mathbf{11_{fc}^{Sc}}$**-qn**$^{\mathbf{Me}}$**-iqn**$^{\mathbf{Me}}$, respectively, upon heating. In the case of $\mathbf{11_{fc}^{Sc}}$**-py**$^{\mathbf{Ph}}$**-pic**, the coupling product $\mathbf{10_{fc}^{Sc}}$**-py**$^{\mathbf{Ph}}$**-pic** could not be isolated because its formation was competitive with its isomerization. Those additional reactions were limited to scandium complexes because mixtures of products that proved intractable were obtained for yttrium and lutetium. Other biheterocyclic complexes $\mathbf{10_{fc}^{M}}$ could be obtained, but the heating of their solutions also gave unsolvable mixtures of products. In some of those mixtures, com-

SCHEME 7. Coupling of η^2-N,C-Imidazolyl Complexes with 2,2′-Bipyridine

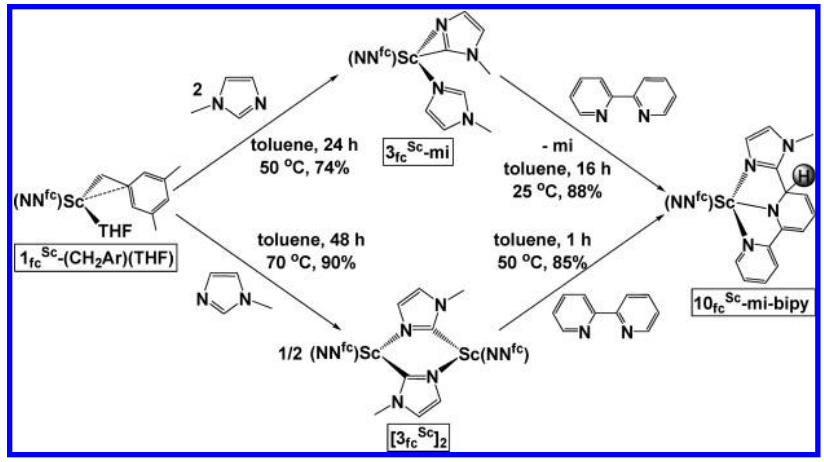

SCHEME 8. Isomerization of Biheterocyclic Ligands in $\mathbf{10_{fc}^{M}}$

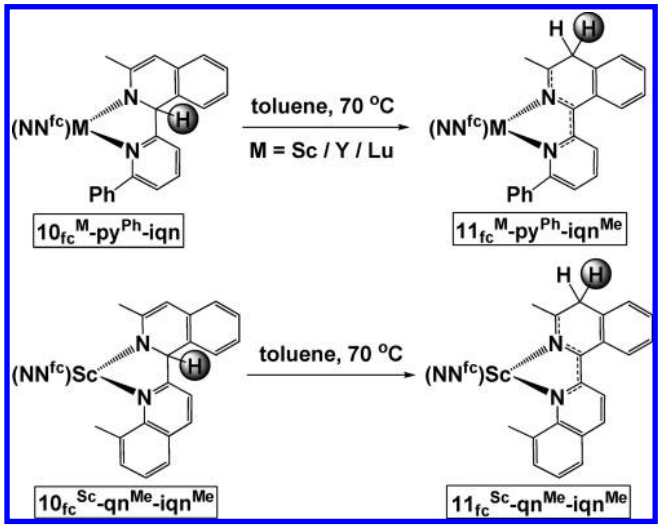

SCHEME 9. Isomerization of the Biheterocyclic Ligand in $\mathbf{10_{fc}^{Sc}}$-$\mathbf{py^{Ph}}$-**bqn**

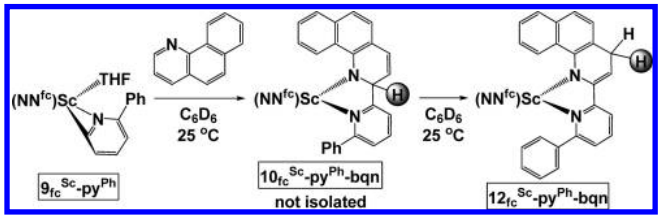

plexes of the type $\mathbf{11_{fc}^{M}}$ could be identified by ^{1}H NMR spectroscopy, but their separation and isolation were not successful.

During the study of the coupling reaction between $\mathbf{9_{fc}^{Sc}}$-$\mathbf{py^{Ph}}$ and 7,8-benzoquinoline, it was found that the coupled product $\mathbf{10_{fc}^{Sc}}$-$\mathbf{py^{Ph}}$-**bqn** formed very slowly (Scheme 9). Before the formation of $\mathbf{10_{fc}^{Sc}}$-$\mathbf{py^{Ph}}$-**bqn** was complete, however, the formation of a second, C_s-symmetric product was observed. The final product was identified as $\mathbf{12_{fc}^{Sc}}$-$\mathbf{py^{Ph}}$-**bqn**, in which the sp^3-hydrogen atom migrated to the benzyl carbon of the dearomatized pyridine ring (Scheme 9).[38] This isomerization reaction is a 1,3- as opposed to a 1,4-hydrogen migration, and it can be explained by the fact that the aromaticity of the naphthalene moiety is preserved in $\mathbf{12_{fc}^{Sc}}$-$\mathbf{py^{Ph}}$-**bqn**.

Mechanistic information was obtained from a crossover experiment between $\mathbf{10_{fc}^{Sc}}$-$\mathbf{qn^{Me}}$-$\mathbf{iqn^{Me}}$-d_4 and $\mathbf{10_{fc}^{Sc}}$-$\mathbf{py^{Ph}}$-$\mathbf{iqn^{Me}}$ (eq 1). The experiment showed that there was no deuterium incorporation into $\mathbf{10_{fc}^{Sc}}$-$\mathbf{py^{Ph}}$-$\mathbf{iqn^{Me}}$, indicating that the isomerization reaction was an intramolecular process. The intramolecular nature of the transformation was also supported by two other observations: (1) reactions in the presence of excess 3-methylisoquinoline did not proceed at a different rate than reactions run in its absence, and (2) the addition of Et_3N to $\mathbf{10_{fc}^{Sc}}$-$\mathbf{qn^{Me}}$-$\mathbf{iqn^{Me}}$ did not influence the rate of the isomerization process.

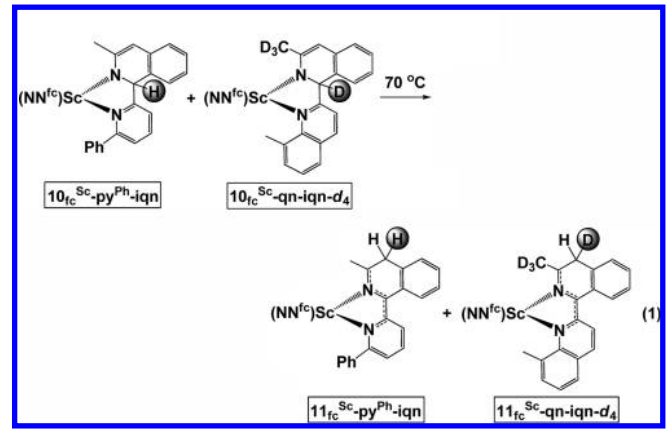

The mechanism for the isomerization of $\mathbf{10_{fc}^{Sc}}$-$\mathbf{py^{Ph}}$-**iqn** to $\mathbf{11_{fc}^{Sc}}$-$\mathbf{py^{Ph}}$-**iqn** was also explored using DFT calculations. It was found that a direct transfer from C2 to C4 was the most energetically favored pathway. The proposed avenue involved a transition structure in which the heterocycle adopted a boat-

like conformation that facilitated the direct proton transfer.[11] DFT calculations were also employed to understand why ring opening was not observed with pyridines, as was the case for other transition metals[22−26] and thorium.[30] Our explanation is based on the stability of the products obtained: we calculated that although the energy of the transition state is in the accessible range, the corresponding product was less stable than the starting material,[11] whereas when the other ring openings occurred the situation was reversed.

3. Reactions with 2,2′-Bipyridine and Isoquinoline.

i. Alkyl Transfer. In an effort to extend the scope of the aromatic N-heterocycle ortho-metalation reaction[10,11,37] to biheterocyclic substrates, the reactions of $\mathbf{1_{fc}^{M}}$-(**CH$_2$Ar**)(**THF**) with 2,2′-bipyridine and isoquinoline were investigated. Instead of the C−H activation reaction encountered with pyridines and imidazoles, products of alkyl transfer to the heterocycle were observed.[12] Such a behavior was reported before for the reaction of Lu(CH$_2$SiMe$_3$)$_3$(THF)$_2$ with 2,2′:6′,2″-terpyridine.[41]

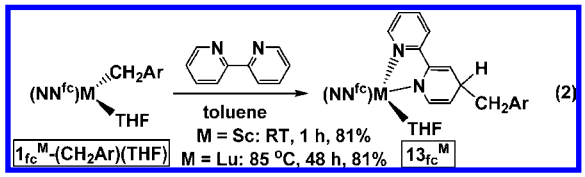

In the case of 2,2′-bipyridine (eq 2), X-ray crystallography indicated that the alkyl transfer occurred to the 4-position of a pyridine ring to give $\mathbf{13_{fc}^{M}}$ (M = Sc).[12] It was proposed that an initial 1,3-alkyl transfer to the 6-position took place, similarly to the 1,3-alkyl transfer from Lu(CH$_2$SiMe$_3$)$_3$(THF)$_2$ to 2,2′:6′,2″-terpyridine,[41] and then an isomerization led to $\mathbf{13_{fc}^{M}}$, likely the thermodynamically stable product.

The reaction of $\mathbf{1_{fc}^{M}}$-(**CH$_2$Ar**)(**THF**) with isoquinoline revealed that a 1,3-alkyl migration of the benzyl group onto the α-carbon of isoquinoline took place at room temperature (M = Y, Lu, La) or 50 °C (M = Sc) resulting in the formation of $\mathbf{14_{fc}^{M}}$-**THF** (Scheme 10). DFT calculations showed that a late transition state was operating for the alkyl-transfer reaction, with the benzyl carbon migrating as a carbanion and almost completely detached from the metal, while the receiving pyridine was partially dearomatized at the potential energy saddle point.

ii. Hydrogen Transfer. During the course of the reaction of $\mathbf{1_{fc}^{M}}$-(**CH$_2$Ar**)(**THF**) with isoquinoline, it was observed that employing an excess of substrate led to the formation of a new product, $\mathbf{15_{fc}^{M}}$-(**iqn**)$_2$, along with 1-benzylisoquinoline, $\mathbf{16^{Ar}}$, through a process of hydrogen transfer (Scheme 10). The hydrogen migration from $\mathbf{14_{fc}^{M}}$-**THF** occurred also to unsaturated substrates with polar double bonds, such as ketones

SCHEME 10. Reactions of Isoquinoline with $\mathbf{1_{fc}^{M}}$-(**CH$_2$Ar**)(**THF**)

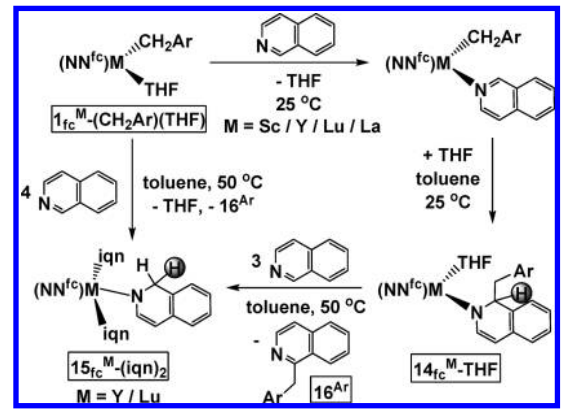

and azobenzene, but it did not take place when 2-butyne, diphenylacetylene, and ethylene were employed. During the study of the latter reactions, it was found that the self transformation of $\mathbf{14_{fc}^{M}}$-**THF** to $\mathbf{15_{fc}^{M}}$-(**THF**)$_2$ and $\mathbf{17_{fc}^{M}}$ occurred (eq 3).[12]

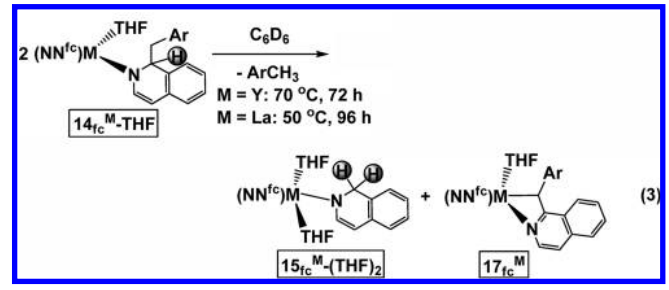

The reaction in eq 3 is somewhat similar to that reported by Cronin et al. for phenanthridinium salts:[42] in the presence of amines, the phenanthridinium salt was dearomatized and a product corresponding to $\mathbf{14_{fc}^{M}}$-**THF** was formed. In the presence of a base, the dearomatized phenanthridinium transferred one proton to a molecule of the initial phenanthridinium salt, leading to the formation of a product corresponding to $\mathbf{15_{fc}^{M}}$-(**THF**)$_2$, and underwent rearomatization, giving a product corresponding to $\mathbf{17_{fc}^{M}}$.

A mechanism for the transformation of $\mathbf{14_{fc}^{M}}$-**THF** to $\mathbf{15_{fc}^{M}}$-(**iqn**)$_2$ was proposed.[12] DFT calculations suggested that a direct transfer of a hydrogen atom between two isoquinoline ligands was the most plausible pathway (eq 4) and that the hydrogen atom migrated as a proton and not as a hydride. The results indicated that the activation barriers in the dearomatization of heterocycles are likely correlated with the lost versus gained aromatic stabilization energy.[12] This pathway was favored over β-hydride elimination.[12] Both types of mechanisms have been proposed to explain the Meerwein−Ponndorf−Verley reduction of ketones by various metal alkoxides,[43] a reaction similar to the transformation of $\mathbf{14_{fc}^{M}}$-**THF** to $\mathbf{15_{fc}^{M}}$-(**iqn**)$_2$.

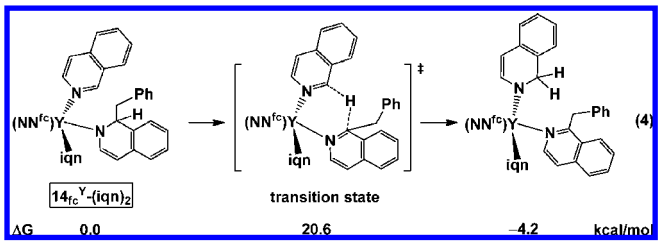

D. Reactions of Alkyl Complexes Supported by a Pyridine−Diamide Ligand

1. DFT Calculations. DFT calculations were employed to probe the iron−metal interaction. Calculations were carried out previously for the scandium and uranium complexes on models in which the Si^{t}Bu$_2$Me group was replaced by SiH$_3$.[9,18] Geometry optimizations on all full structures were performed, and these results are reported here. The validity of the calculations was established by comparing calculated metrical parameters with those from the corresponding X-ray crystal structures. Although the optimized iron−metal distance compares well to the experimental parameter for most complexes in the series (Table 3), this is not the case for yttrium (entry 3) and two lutetium (entries 4 and 6) complexes. The following parameters are discussed: (1) the Mayer bond orders and (2) the Hirshfeld charge of the central metal and of the carbon bound to it (Table 3, see the Supporting Information for other parameters).

Mayer bond orders for the metal−iron interaction are small for group 3 metals (entries 1−7) and become significant only for uranium (entries 8, 9). It is important to point out that these values are similar to those calculated for the bond between the group 3 metal and the ether-oxygen donor (ca. 0.2). With the exception of the uranium complexes (entries 8−9), the calculated bond order for the metal−iron interaction varies only slightly with the nature of the metal center in benzyl complexes (entries 1, 3, 4, and 7). For the same metal center, the bond order is dependent on the nature of the ligands present: the more electron donating the ligands, the weaker the metal−iron interaction. This effect is seen when the nonferrocene ligands are modified (entries 1 and 2) or when the electronic properties of the nitrogen donor are changed (entries 4, 5).

Although the trend observed with metal Hirshfeld charges needs to be verified by experimental data, it is interesting to note that these values increase in the order Sc < La < Y < Lu, which is not the order expected based on their Lewis acidities (Bader charges vary in the order Sc < Lu < Y < La, see the Supporting Information).[44] These differences are small and because geometry optimizations of key structures did not yield a good agreement with the experimental metal−iron distances, a rigorous interpretation of the variation in calculated charges is not attempted here. For the same series of benzyl complexes, the charge on the benzyl carbon atom is almost unchanged.

From a geometrical point of view, 1,1′-ferrocenenylene−diamides resemble pincer diamides. DFT calculations carried out on full structures for pyridine−diamide yttrium and lutetium benzyl complexes show that both the Mayer bond orders for the N$_{py}$−metal interaction (0.19 for Y, 0.26 for Lu) and the Hirshfeld charges vary surprisingly little (0.58 for Y, 0.58 for Lu) compared with the analogous values in the ferrocene−diamide complexes (Table 3). Based on these results, we expected to see the reactions of the pyridine−diamide complexes toward aromatic N-heterocycles manifest similarly to those of the ferrocene−diamide complexes and set out to determine their scope.

2. Reactions with 1-Methylimidazole. The reaction between **1$_{py}^{Y}$-(CH$_2$Ph)(THF)** or **1$_{py}^{Lu}$-(CH$_2$Ar)(THF)** and 3 equiv of 1-methylimidazole (eq 5) resulted in the formation **2$_{py}^{M}$-mi**, analogously to what was observed for the ferrocene-based complexes.[14] We proposed that a similar mechanism operated in those transformations as well. The reactions with 1-methylbenzimidazole, however, did not proceed cleanly for the pyridine−diamide complexes.

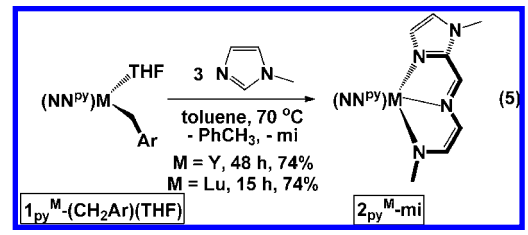

3. Reactions with Pyridines. The reaction between **1$_{py}^{M}$-(CH$_2$Ar)(THF)** and 4 equiv of pyridine at 50 °C gave a mixture of products, similarly to what was observed when the corresponding ferrocene−diamide complexes were employed. Unlike the case for **1$_{fc}^{M}$-(CH$_2$Ar)(THF)** though, the reactions between **1$_{py}^{M}$-(CH$_2$Ar)(THF)** and 2-phenylpyridine or 8-methylquinoline also resulted in intractable mixtures of products.[14]

A reaction sequence analogous to that observed for the ferrocene−diamide complexes was found only when 2-picoline was employed to give **9$_{py}^{M}$-pic**, followed by the coupling with 3-methylisoquinoline to form the expected biheterocyclic product **10$_{py}^{M}$-pic-iqn^{Me}**, in which the heterocyclic ring of 3-methylisoquinoline was dearomatized (Scheme 11).[14] Other C−C coupling reactions were not successful.

TABLE 3. DFT Calculated Parameters for d^0f^n Alkyl Complexes

entry	complex	calcd (X-ray) Fe−M distance (Å)	Fe−M bond order[a]	Hirshfeld charge of M	Hirshfeld charge of C_{Bz}
1	$\mathbf{1_{fc}^{Sc}}$-(**CH$_2$Ar**)(**THF**)	3.18 (3.16)	0.22	0.49	−0.24
2	$\mathbf{1_{fc}^{Sc}}$-**Me**(**THF**)$_2$	3.38 (3.26)	0.13	0.46	−0.31
3	$\mathbf{1_{fc}^{Y}}$-(**CH$_2$Ph**)(**THF**)	3.33 (3.24)	0.22	0.56	−0.23
4	$\mathbf{1_{fc}^{Lu}}$-(**CH$_2$Ar**)(**THF**)	3.32 (3.25)	0.19	0.59	−0.24
5	$\mathbf{1_{Ad}^{Lu}}$-(**CH$_2$Ar**)(**DME**)	3.36 (3.34)	0.17	0.59	−0.24
6	$\mathbf{1_{Mes}^{Lu}}$-(**CH$_2$Ar**)(**THF**)	3.36 (3.12)	0.17	0.60	−0.24
7	$\mathbf{1_{fc}^{La}}$-(**CH$_2$Ar**)(**THF**)	3.41 (3.38)	0.21	0.53	−0.23
8	$\mathbf{1_{fc}^{U}}$-(**CH$_2$Ph**)$_2$	3.20 (3.19)	0.39	0.64	−0.22, −0.21
9	$\mathbf{1_{fc}^{U}}$-(**CH$_2$Ph**)(**OEt$_2$**)	3.12 (3.07)	0.49	0.71	−0.21

[a] Mayer bond orders.

SCHEME 11. Reactions of $\mathbf{1_{py}^{M}}$-(**CH$_2$Ar**)(**THF**) with 2-Picoline and Subsequent C−C Coupling Reactions with 3-Methylisoquinoline

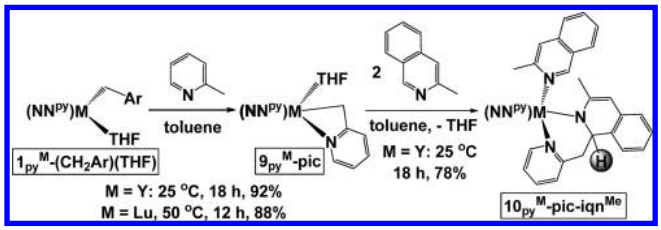

SCHEME 12. Reactions of Isoquinoline with $\mathbf{1_{py}^{M}}$-(**CH$_2$Ar**)(**THF**)

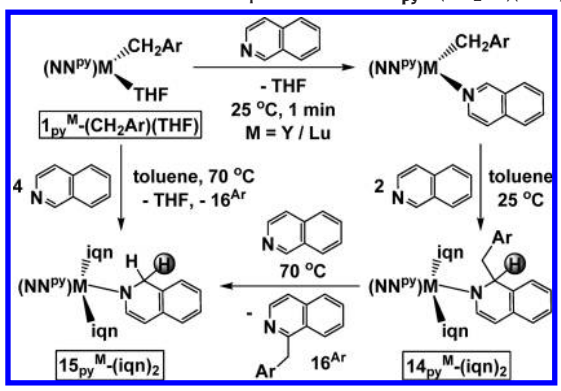

4. Reactions with Isoquinoline. The complexes $\mathbf{1_{py}^{M}}$-(**CH$_2$Ar**)(**THF**) reacted with 3 equiv of isoquinoline in toluene at room temperature to give $\mathbf{14_{py}^{M}}$-(**iqn**)$_2$ (Scheme 12). When toluene solutions of $\mathbf{1_{py}^{M}}$-(**CH$_2$Ar**)(**THF**) and 4 equiv of isoquinoline were heated at 70 °C, the products $\mathbf{15_{py}^{M}}$-(**iqn**)$_2$ were isolated. Both reactions are analogous to those described for the ferrocene−diamide complexes.

E. Conclusions

1,1′-Ferrocene−diamide complexes of group 3 metals and uranium showed a diverse array of reactivity with aromatic N-heterocycles. The reactions of benzyl complexes were investigated, and a substrate-dependent behavior was observed. For example, 1-methylimidazole was cleaved by all the metal complexes studied. With pyridines, subtle differences were identified: C−H activation and C−C coupling were operative for ortho-substituted pyridines, while alkyl transfer was manifested for isoquinoline and chelating pyridines. The products of the C−C coupling or the alkyl-transfer reactions were found to undergo hydrogen transfer subsequently: within the same ring for the former and between two different heterocycles for the latter.

The comparison between the ferrocene− and pyridine−diamide benzyl complexes showed that similar reactions were observed with 1-methylimidazole, 2-picoline, and isoquinoline. It is important to note, however, that other types of reactions and a larger substrate scope were identified for the ferrocene- than for the pyridine-based complexes.

Although some of the reactions observed with the ferrocene−diamide group 3 metal benzyl complexes have been previously reported for other classes of compounds, those examples were isolated and, in some cases, the reactions were not straightforward. In this light, the ferrocene diamides represent a versatile ligand framework. This finding is significant because the analysis of different reactivity behaviors with one class of complexes allowed comparisons to be made and factors leading to individual reactions to be rationalized. It is possible that the privileged status of these organometallic ancillary ligands is a consequence of iron's ability to accommodate changes in the electronic density at the metal center more readily than classical supporting ligands can.

The efforts of present and former members of the Diaconescu laboratory were crucial in making this project possible. Their names, together with those of valuable collaborators, appear in the references from which this Account draws. Ohyun Kwon, UCLA, and Parisa Mehrkhodavandi, University of British Columbia, Vancouver, are acknowledged for helpful discussions. The research summarized herein has been funded by the UCLA, UC Energy Institute, DOE (Grant ER15984), Sloan Foundation, and NSF (Grant CHE-0847735).

Supporting Information Available. X-ray crystal structure of 1_{Mes}^{Lu}-(CH_2Ar)(THF), including CIF, DFT details and parameters, and calculated coordinates for all compounds. This material is available free of charge via the Internet at http://pubs.acs.org.

BIOGRAPHICAL INFORMATION

Paula Diaconescu joined the UCLA Chemistry & Biochemistry department in 2005 after spending two years as a postdoctoral fellow in the group of Prof. Robert Grubbs at California Institute of Technology. She obtained her Ph.D. degree under the supervision of Prof. Christopher Cummins at Massachusetts Institute of Technology working on arene-bridged complexes of uranium. Her earlier education was completed in Romania, where she obtained her B.Sc. from the University of Bucharest and worked on coordination complexes of transition metals and lanthanides at the University Politehnica of Bucharest. Her current research efforts focus on the design of reactive metal complexes with applications to small molecule activation, organic synthesis, and polymer formation.

FOOTNOTES

*E-mail: pld@chem.ucla.edu.

REFERENCES

1 Chinchilla, R.; Najera, C.; Yus, M. Metalated Heterocycles and Their Applications in Synthetic Organic Chemistry. *Chem. Rev.* **2004**, *104*, 2667–2722.

2 Sanchez-Delgado, R. A. *Organometallic Modelling of the Hydrodesulfurization and Hydrodenitrogenation Reactions*; Kluwer Academic Publishers: Dordrecht, the Netherlands, 2002.

3 Diaconescu, P. L. Reactions of Early Transition Metal-Carbon Bonds with N-Heterocycles. *Curr. Org. Chem.* **2008**, *12*, 1388–1405.

4 Chirik, P. J.; Wieghardt, K. Radical Ligands Confer Nobility on Base-Metal Catalysts. *Science* **2010**, *327* (5967), 794–795.

5 Shafir, A.; Power, M. P.; Whitener, G. D.; Arnold, J. Silylated 1,1′-diaminoferrocene: Ti and Zr complexes of a new chelating diamide ligand. *Organometallics* **2001**, *20* (7), 1365–1369.

6 Shafir, A.; Arnold, J. Stabilization of a Cationic Ti Center by a Ferrocene Moiety: A Remarkably Short Ti−Fe Interaction in the Diamide $\{[(\eta^5\text{-}C_5H_4NSiMe_3)_2Fe]TiCl\}_2^{2+}$. *J. Am. Chem. Soc.* **2001**, *123* (37), 9212–9213.

7 Seyferth, D.; Hames, B. W.; Rucker, T. G.; Cowie, M.; Dickson, R. S. A Novel Palladium Complex with Iron−Palladium Dative Bonding Derived from 1,2,3-Trithia[3]ferrocenophane, $(Ph_3P)PdFe(SC_5H_4)_2 \cdot 0.5C_6H_5CH_3$. *Organometallics* **1983**, *2*, 472–474.

8 Ramos, A.; Otten, E.; Stephan, D. W. Stabilizing Zr and Ti Cations by Interaction with a Ferrocenyl Fragment. *J. Am. Chem. Soc.* **2009**, *131*, 15610–15611.

9 Carver, C. T.; Monreal, M. J.; Diaconescu, P. L. Scandium Alkyl Complexes Supported by a Ferrocene Diamide Ligand. *Organometallics* **2008**, *27*, 363–370.

10 Carver, C. T.; Diaconescu, P. L. Ring-Opening Reactions of Aromatic N-Heterocycles by Scandium and Yttrium Alkyl Complexes. *J. Am. Chem. Soc.* **2008**, *130*, 7558–7559.

11 Carver, C. T.; Benitez, D.; Miller, K. L.; Williams, B. N.; Tkatchouk, E.; Goddard, W. A.; Diaconescu, P. L. Reactions of Group III Biheterocyclic Complexes. *J. Am. Chem. Soc.* **2009**, *131*, 10269–10278.

12 Miller, K. L.; Williams, B. N.; Benitez, D.; Carver, C. T.; Ogilby, K. R.; Tkatchouk, E.; Goddard, W. A.; Diaconescu, P. L. Dearomatization Reactions of N-Heterocycles Mediated by Group 3 Complexes. *J. Am. Chem. Soc.* **2010**, *132*, 342–355.

13 Wong, A. W.; Miller, K. L.; Diaconescu, P. L. Reactions of Aromatic N-Heterocycles with a Lutetium Benzyl Complex Supported by a Ferrocene-Diamide Ligand. *Dalton Trans.* **2010**, *39*, 6726–6731.

14 Jie, S.; Diaconescu, P. L. Reactions of Aromatic N-Heterocycles with Yttrium and Lutetium Benzyl Complexes Supported by a Pyridine-Diamide Ligand. *Organometallics* **2010**, *29* (5), 1222–1230.

15 Bambirra, S.; Meetsma, A.; Hessen, B. Lanthanum Tribenzyl Complexes as Convenient Starting Materials for Organolanthanum Chemistry. *Organometallics* **2006**, *25* (14), 3454–3462.

16 Piers, W. E.; Emslie, D. J. H. Non-cyclopentadienyl Ancillaries in Organogroup 3 Metal Chemistry: A Fine Balance in Ligand Design. *Coord. Chem. Rev.* **2002**, *233–234*, 131–155.

17 Wooles, A. J.; Mills, D. P.; Lewis, W.; Blake, A. J.; Liddle, S. T. Lanthanide Tribenzyl Complexes: Structural Variations and Useful Precursors to Phosphorus-Stabilised Lanthanide Carbenes. *Dalton Trans.* **2010**, *39* (2), 500–510.

18 Monreal, M. J.; Diaconescu, P. L. A Weak Interaction between Iron and Uranium in Uranium Alkyl Complexes Supported by Ferrocene Diamide Ligands. *Organometallics* **2008**, *27*, 1702–1706.

19 Duhovic, S.; Khan, S.; Diaconescu, P. L. In Situ Generation of Uranium Alkyl Complexes. *Chem. Commun.* **2010**, *46* (19), 3390–3392.

20 Cordero, B.; Gomez, V.; Platero-Prats, A. E.; Reves, M.; Echeverria, J.; Cremades, E.; Barragan, F.; Alvarez, S. Covalent Radii Revisited. *Dalton Trans.* **2008**, (21), 2832–2838.

21 Jordan, R. F.; Guram, A. S. Scope and Regiochemistry of Ligand Carbon−Hydrogen Activation Reactions of $Cp_2Zr(CH_3)(THF)^+$. *Organometallics* **1990**, *9* (7), 2116–2123.

22 Allen, K. D.; Bruck, M. A.; Gray, S. D.; Kingsborough, R. P.; Smith, D. P.; Weller, K. J.; Wigley, D. E. Quinoline Binding Mode as a Function of Oxidation State in Aryloxide-Supported Tantalum Complexes: Models for Hydrodenitrogenation Catalysis. *Polyhedron* **1995**, *14* (22), 3315–3333.

23 Kleckley, T. S.; Bennett, J. L.; Wolczanski, P. T.; Lobkovsky, E. B. Pyridine C═N Bond Cleavage Mediated by $(silox)_3Nb$ (silox = $^t Bu_3SiO$). *J. Am. Chem. Soc.* **1997**, *119* (1), 247–248.

24 Neithamer, D. R.; Parkanyi, L.; Mitchell, J. F.; Wolczanski, P. T. η^2-(N,C)-Pyridine and μ-η^2(1,2):η^2(4,5)-Benzene Complexes of $(silox)_3Ta$ (silox = *t*-Bu_3SiO-). *J. Am. Chem. Soc.* **1988**, *110* (13), 4421–4423.

25 Fout, A. R.; Bailey, B. C.; Tomaszewski, J.; Mindiola, D. J. Cyclic Denitrogenation of N-Heterocycles Applying a Homogeneous Titanium Reagent. *J. Am. Chem. Soc.* **2007**, *129* (42), 12640–12641.

26 Bailey, B. C.; Fan, H.; Huffman, J. C.; Baik, M. H.; Mindiola, D. J. Room Temperature Ring-Opening Metathesis of Pyridines by a Transient TiC Linkage. *J. Am. Chem. Soc.* **2006**, *128* (21), 6798–6799.

27 Huertos, M. A.; Perez, J.; Riera, L. Pyridine Ring Opening at Room Temperature at a Rhenium Tricarbonyl Bipyridine Complex. *J. Am. Chem. Soc.* **2008**, *130* (17), 5662–5663.

28 Huertos, M. A.; Peérez, J.; Riera, L.; Meneéndez-Velaázquez, A. From N-Alkylimidazole Ligands at a Rhenium Center: Ring Opening or Formation of NHC Complexes. *J. Am. Chem. Soc.* **2008**, *130* (41), 13530–13531.

29 Sattler, A.; Parkin, G. Cleaving Carbon-Carbon Bonds by Inserting Tungsten into Unstrained Aromatic Rings. *Nature* **2010**, *463*, 523–526.

30 Pool, J. A.; Scott, B. L.; Kiplinger, J. L. Carbon-Nitrogen Bond Cleavage in Pyridine Ring Systems Mediated by Organometallic Thorium(IV) Complexes. *Chem. Commun.* **2005**, (20), 2591–2593.

31 Arunachalampillai, A.; Crewdson, P.; Korobkov, I.; Gambarotta, S. Ring Opening and C−O and C−N Bond Cleavage by Transient Reduced Thorium Species. *Organometallics* **2006**, *25*, 3856–3866.

32 Deelman, B.-J.; Stevels, W. M.; Teuben, J. H.; Lakin, M. T.; Spek, A. L. Insertion Chemistry of Yttrium Complex Cp^*_2Y(2-pyridyl) and Molecular Structure of an Unexpected CO Insertion Product $(Cp^*_2Y)_2(\mu\text{-}\eta^2\text{:}\eta^2\text{-}OC(NC_5H_4)_2)$. *Organometallics* **1994**, *13* (10), 3881–3891.

33 Miller, K. L.; Carver, C. T.; Williams, B. N.; Diaconescu, P. L. Reactions of Imidazoles with Electrophilic Metal Alkyl Complexes. *Organometallics* **2010**, *29*, 2272–2281.

34 Monreal, M. J.; Khan, S.; Diaconescu, P. L. Beyond C-H Activation with Uranium: A Cascade of Reactions Mediated by a Uranium Dialkyl Complex. *Angew. Chem., Int. Ed.* **2009**, *48* (44), 8352–8355.

35 Duhović, S.; Monreal, M. J.; Diaconescu, P. L. Reactions of Aromatic Heterocycles with Uranium Alkyl Complexes. *Inorg. Chem.* **2010**, DOI: 10.1021/ ic.1009835.

36 Monreal, M. J.; Diaconescu, P. L. Reversible C-C Coupling in a Uranium Biheterocyclic Complex. *J. Am. Chem. Soc.* **2010**, *132*, 7676–7683.

37 Carver, C. T.; Diaconescu, P. L. Insertion Reactions of Scandium Pyridyl Complexes Supported by a Ferrocene Diamide Ligand. *J. Alloys Compd.* **2009**, *488*, 518–523.

38 Carver, C. T.; Williams, B. N.; Ogilby, K. R.; Diaconescu, P. L. Coupling of Aromatic N-Heterocycles Mediated by Group 3 Complexes. *Organometallics* **2010**, *29* (4), 835–846.

39 Duchateau, R.; Brussee, E. A. C.; Meetsma, A.; Teuben, J. H. Synthesis and Reactivity of Bis(alkoxysilylamido)yttrium η^2-Pyridyl and η^2-α-Picolyl Compounds. *Organometallics* **1997**, *16*, 5506–5516.

40 Kiplinger, J. L.; Scott, B. L.; Schelter, E. J.; Pool Davis Tournear, J. A. sp^3 versus sp^2 C-H Bond Activation Chemistry of 2-Picoline by Th(IV) and U(IV) Metallocene Complexes. *J. Alloys Compd.* **2007**, *444−445*, 477–482.

41 Jantunen, K. C.; Scott, B. L.; Hay, P. J.; Gordon, J. C.; Kiplinger, J. L. Dearomatization and Functionalization of Terpyridine by Lutetium(III) Alkyl Complexes. *J. Am. Chem. Soc.* **2006**, *128*, 6322–6323.

42 Parenty, A. D. C.; Smith, L. V.; Pickering, A. L.; Long, D.-L.; Cronin, L. General One-Pot, Three-Step Methodology Leading to an Extended Class of N-Heterocyclic Cations: Spontaneous Nucleophilic Addition, Cyclization, and Hydride Loss. *J. Org. Chem.* **2004**, *69*, 5934–5946.

43 Cha, J. S. Recent Developments in Meerwein−Ponndorf−Verley and Related Reactions for the Reduction of Organic Functional Groups Using Aluminum, Boron, and Other Metal Reagents: A Review. *Org. Process Res. Dev.* **2006**, *10*, 1032–1053.

44 Tsuruta, H.; Imamoto, T.; Yamaguchi, K. Evaluation of the Relative Lewis Acidities of Lanthanoid(III) Compounds by Tandem Mass Spectrometry. *Chem. Commun.* **1999**, 1703–1704.